Internal friction associated with grain boundaries in Ni-Cr alloys*

B. Cao, R. Schaller and W. Benoit

Ecole Polytechnique Fédérale de Lausanne, Institut de Génie Atomique, CH-1015 Lausanne (Switzerland)

F. Cosandey

The State University of New Jersey, Rutgers, Department of Mechanics and Materials Science, PO Box 909, Piscataway, NJ 08854 (USA)

Abstract

The internal friction spectrum of Ni–20at.%Cr polycrystals is mainly characterized by two relaxation peaks: P1 at about 950 K upon heating; P3 peak at about 1100 K upon cooling, respectively, and a large hysteresis in the peak P3 temperature range. Under some experimental conditions, another peak (P2) is also observed during heating in the temperature range higher than peak P1. In an Ni–20at.%Cr single crystal, only peak P1 is observed during heating and cooling. However, when the single crystal is recrystallized, an internal friction spectrum identical to that of the polycrystal is observed. Furthermore, metallographical observations show that the large hysteresis in internal friction is related to the presence of discrete carbide precipitates at grain boundaries. When the grain boundary is free of carbide precipitates, only peak P3 is observed during the heating and cooling run. In contrast, when the grain boundary contains a continuous distribution of carbide precipitates, only peak P1 is observed during the heating and cooling run. This experimental evidence leads us to attribute peak P3 to grain boundary relaxation, which is affected by the carbide precipitates, and peak P1 to a relaxation process taking place in the grains. The hysteresis results from the dissolution–precipitation processes of grain boundary carbides.

1. Introduction

The high temperature deformation and fracture behaviour of polycrystalline materials are strongly affected by the presence of both grain boundaries and impurities. A creep rupture phenomenon occurs often by the formation, growth and interlinkage of grain boundary microcracks and cavities [1, 2]. It is generally believed that grain boundary sliding is an essential process which causes stress concentration and, hence, cavity nucleation at obstacles along the boundary, such as triple points, ledges and second-phase particles [1–4]. Accordingly, the study of the structure and mobility of grain boundaries is highly important for the understanding of the high temperature behaviour of materials. However, information on movements on an atomic scale cannot normally be obtained from conventional grain boundary sliding studies, but can be obtained by internal friction measurements [5].

Phenomenologically, grain boundaries slide in a viscous manner under a shear stress field. This process manifests itself in an anelastic deformation and then in internal friction [6–8]. In the earliest work of Kê [7] in aluminium, a relaxation peak in the high tem-

perature range was attributed to grain boundary sliding, since the grain boundary internal friction has been studied in a wide range of materials [9, 10]. However, further internal friction experiments have led to additional models for the basic mechanism of high temperature relaxation, such as grain boundary migration [11], the movement of grain boundary dislocations [12–14] and lattice dislocations [15]. At present, the detailed mechanism is not well known, and even the controversy about the origin of the high temperature relaxation is still not completely resolved [16].

Our previous internal friction results on commercial Ni–Cr–Ce alloys revealed some anelastic phenomena, which could be related to the grain boundaries [17–20]. In this paper, we report further results of high temperature internal friction measurements for pure Ni–Cr alloys. The evolution of the high temperature relaxation peak, in relation to the grain boundary microstructure, leads us to attribute the origin of the peak to grain boundary sliding.

2. Experimental procedure

Ni–Cr alloys were prepared with high purity nickel (99.99%) and chromium (99.996%) by the Institute of

---

*Invited paper.

Applied Physics, Swiss Federal Institute of Technology (ETH), Zürich. Polycrystalline alloys with compositions of 20 and 33 at.% Cr were prepared by vacuum induction melting followed by casting. Single-crystal alloys with compositions of 22 and 33 at.% Cr were grown by the Bridgman technique in an alumina crucible.

The specimens for the internal friction measurements were spark machined in the form of thin bars 110 (or 60) mm×2.5 mm×0.5 mm. Before the measurements, all the polycrystalline specimens were vacuum annealed for 10 min at 1323 K to obtain a consistently similar grain size of about 80 μm, and were then aged under vacuum for 24 h at 1200 K to stabilize the microstructure. The single crystals were verified by electrolytic etching and Laue X-ray analysis, and then annealed at 1200 K to eliminate any possible handling effects before the measurement.

The internal friction measurements were carried out at low frequency by the free-decay technique in a computer-controlled inverted torsion pendulum [21]. The measurements were made on heating and cooling between room temperature and 1273 K at a rate of 2 K min^{-1}, with a maximum strain amplitude of 3×10^{-5}. The measurements were performed in a vacuum of 5×10^{-5} Torr or better, except for the study of oxygen effects on high temperature internal friction, where the vacuum was 5×10^{-4} Torr or less.

3. Results

A typical internal friction spectrum as a function of temperature for the alloy Ni-20at.%Cr is shown in Fig. 1. It is mainly characterized by two internal friction peaks, marked P1 and P3, upon heating and cooling, respectively, as well as a large hysteresis in the temperature range peak P3. During heating, the first peak (P1) superimposed on a high temperature background
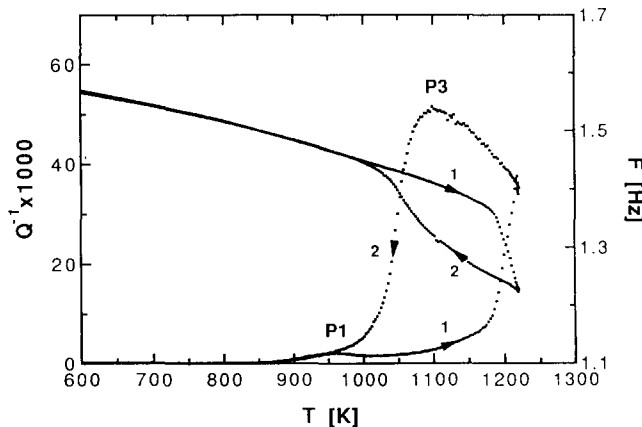
appears at about 950 K. A sharp increase in the internal friction background occurs at about 1185 K, which is accompanied by a large drop in frequency. For some experimental conditions, another peak (P2) is also observed during heating in the temperature range higher than peak P1 (cf. Fig. 8, later). Since the dynamic shear modulus G is proportional to the square of the frequency, this decrease in frequency is indicative of a softening of the alloy. Upon cooling, the background remains high and peak P3 occurs at about 1100 K. This peak is followed by a rapid decrease in the internal friction, as well as a recovery in frequency. Because it happens in the P1 peak temperature range, it is difficult to recognize the presence of peak P1 upon cooling.

The effect of the vibration frequency on the internal friction spectrum is presented in Fig. 2. The peak temperatures of peaks P1 and P3 both shift to higher temperatures with increasing frequency. This means that the phenomena responsible for the peaks are thermally activated. However, the sharp increase and the rapid decrease in internal friction during the thermal cycles seem not to be sensitive to the changes in the frequency. This is indicative of non-thermally activated phenomena, such as phase transformation processes. The activation energy for the relaxation process of peak P1 deduced from the Arrhenius plot, is 2.92 eV. It is then very close to the activation energies of lattice diffusion of Ni (2.96 eV) and Cr (2.94 eV) in Ni-20at.% Cr alloy [22]. In the case of peak P3, it is difficult to subtract a high temperature background as in the case of peak P1. In addition, the peak is obviously affected by the frequency-independent decrease in the internal friction upon cooling. Consequently, the activation energy cannot be precisely determined in this case.

To localize the origin of these two relaxation peaks, internal friction measurements have been performed in Ni-20at.%Cr single crystals. In this case, only the P1 peak is observed, at the same temperature and with

Fig. 1. Internal friction Q^{-1} and frequency F measured on (1) heating and (2) cooling vs. temperature of Ni-20at.%Cr polycrystals.
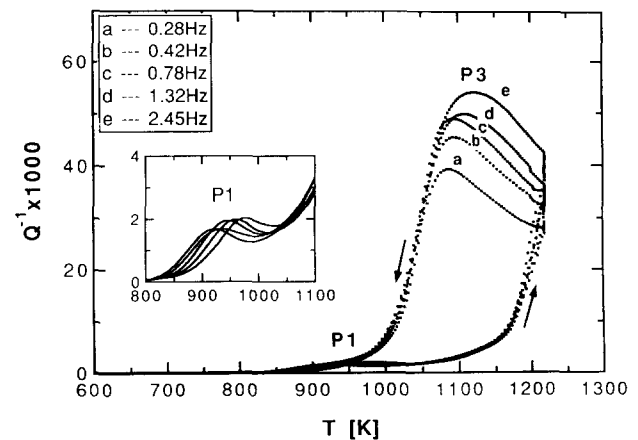

Fig. 2. Effect of the frequency on internal friction spectrum of Ni-20at.%Cr polycrystals.

a similar peak height as in the polycrystalline alloy, during heating as well as during cooling (Fig. 3). The activation energy for peak P1 is found to be 2.87 eV.

These results lead us to suggest that the origin of peak P1 may be within the grains, and that peak P3 and the large hysteresis may be related to the presence of grain boundaries.

In proposing the above assumptions, it is interesting to survey the evolution of the internal friction spectrum during the transition from a single-crystal to a polycrystalline state. The two following experiments have been carried out. First, the internal friction spectrum of Ni–20at.%Cr single crystals was measured (Fig. 4, curves 1 and 2). The specimen was then cold rolled at room temperature by about 12%. The specimen was measured again in the pendulum. The first heating is shown by curve 3 in Fig. 4. After annealing for 6 h at 1200 K to recrystallize and stabilize the structure,
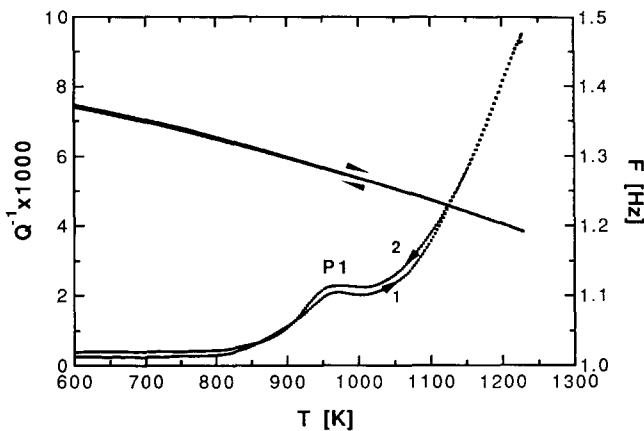

Fig. 3. Internal friction Q^{-1} and frequency F measured on (1) heating and (2) cooling vs. temperature of Ni–20at.%Cr single crystals.
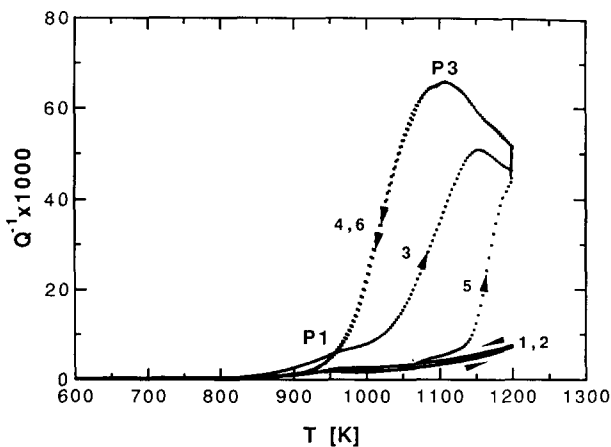

Fig. 4. Evolution of the internal friction spectrum of an Ni–20at.%Cr single crystal (1, 2) initial state; (3) the heating run after cold rolling by about 12% at room temperature and (4) the cooling run after annealing for 6 h at 1200 K; (5) subsequent heating and (6) cooling run.

peak P3 appeared immediately upon cooling (Fig. 4, curve 4). During the subsequent thermal cycles, an internal friction spectrum identical to that of the polycrystal was observed (Fig. 4, curves 5 and 6). In another experiment, the specimen was cold rolled successively up to 12%, and internal friction measurements were performed after each cold rolling. Then, the evolution of the spectrum from that of a single crystal to a polycrystal was clearly observed. Metallographical observations on these two specimens confirmed both that the recrystallization was taking place when peak P3 was appearing, and showed also the presence of discrete carbide precipitates at the grain boundaries.

From this experimental evidence, it is possible to conclude that peak P3 and the large hysteresis are associated with the grain boundaries, and that peak P1 is related to a relaxation process taking place in the interior of the grains. A recent detailed analysis revealed that peak P1 may be related to a Zener relaxation process [23].

3.1. Effect of the grain boundary precipitates

To understand the evolution of the internal friction spectrum with temperature and, in particular, the hysteresis, a detailed microstructural analysis by transmission electron microscopy (TEM) and scanning electron microscopy (SEM) was performed [18, 19]. It was shown that the sharp increase in internal friction corresponds to the critical temperature of the dissolution of the grain boundary carbides of the form Cr_7C_3. A microstructural analysis, performed on the specimen which gave the internal friction spectrum in Fig. 1, revealed the presence of discrete carbide particles with sizes of about 1 μm. The results showed clearly that the carbides dissolve completely at 1200 K and precipitate during subsequent cooling. Therefore, the internal friction hysteresis should be associated with the dissolution on heating and precipitation on cooling of the grain boundary carbides Cr_7C_3, which correspond to the sharp increase and the rapid decrease in internal friction respectively.

Furthermore, to determine the effect of grain boundary precipitates on the conditions of the appearance of peak P3 and on the hysteresis, internal friction measurements were performed on specimens with a specific grain boundary structure. Figure 5 shows the internal friction spectrum of an Ni–10at.%Cr alloy, which do not contain any grain boundary carbides. A stable peak P3 was observed during heating and cooling, with an activation energy of 2.7 eV. The hysteresis and peak P1 were absent. This is an indication that the observed hysteresis is strictly related to the presence of the precipitates at grain boundaries. The internal friction spectrum was also measured in Ni–20at.%Cr after annealing for 15 min at 1383 K, followed by 24
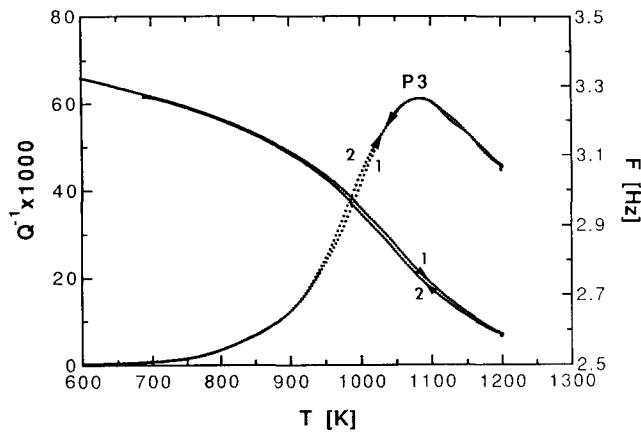
Fig. 5. Internal friction Q^{-1} and frequency F measured on (1) heating and (2) cooling vs. temperature of Ni–10at.%Cr polycrystals.
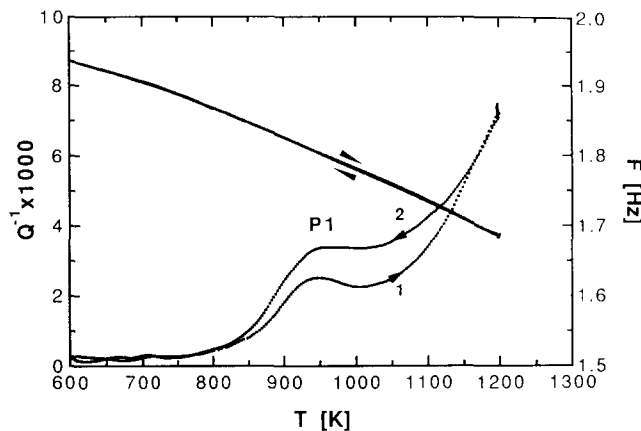

Fig. 6. Internal friction Q^{-1} and frequency F measured on (1) heating and (2) cooling vs. temperature of Ni–20at.%Cr polycrystals after annealing for 15 min at 1373 K and then for 24 h at 1200 K.

Fig. 7. Internal friction Q^{-1} measured on (1) heating and (2) cooling vs. temperature on (a) Ni–20at.%Cr and (b) Ni–33at.%Cr polycrystalline alloys.

h at 1200 K. The specimen then contains a continuous distribution of grain boundary carbide precipitates. In this case, only peak P1 was observed, with a little hysteresis during the heating and cooling cycles, and peak P3 did not appear (Fig. 6). This spectrum is very similar to that of a single crystal (Fig. 3).

3.2. Effect of the concentration of chromium

The internal friction spectra in Ni–33at.%Cr alloys, in both single-crystal and polycrystal forms, are similar to those of Ni–20at.%Cr. The internal friction spectra of the polycrystalline alloys are shown in Fig. 7. The temperature of peaks P1 and P3 both shift to higher temperatures with increasing chromium content, but the peak height of peak P3 is clearly decreased. In addition, the critical temperature corresponding to the dissolution and precipitation process seems to appear at a slightly higher temperature in Ni–33at.%Cr than in Ni–20at.%Cr. The shift of the peak temperature
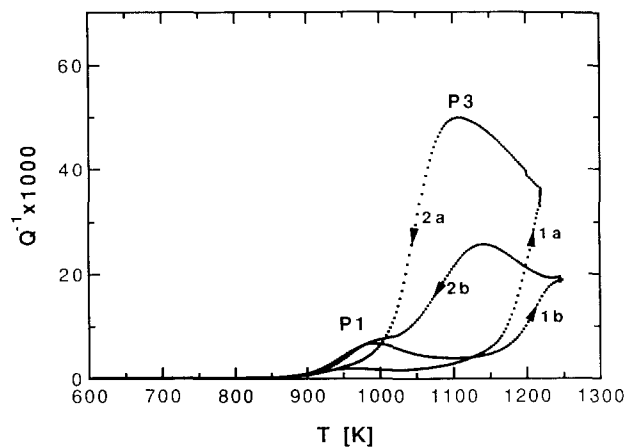
may result from the dependence of the activation energy on the solute concentration, because the energy of lattice diffusion increases with the solute concentration in the Ni–Cr system. If peak P3 is related to a relaxation process at grain boundaries, the changes in peak P3 caused by increasing chromium may be related to the change in grain boundary diffusivity and also to the concentration of solute atoms in and near the grain boundaries.

3.3. Effect of oxygen on internal friction spectrum

It is known that, in nickel and nickel alloys, oxygen penetration along grain boundaries can lead to a reaction with the carbides present at the grain boundaries. That reaction dissolves the carbides, forming CO and CO_2 [24, 25]. In a previous investigation [20], internal friction measurements were performed in Ni–22at.%Cr–Ce in an oxygen-contaminated environment (i.e. a vacuum of over 5×10^{-4} Torr). A continuous attenuation of the internal friction hysteresis between heating and cooling cycles was observed. As a result, a new stable internal friction spectrum was observed after about 20 cycles, which was characterized by a stabilized peak P3 upon heating and cooling.

To identify further the effect of oxygen on the internal friction spectrum, a specimen of Ni–22at.%Cr alloy was pre-oxidized in air for 1 h at 973 K, then measured in the same environments as in the previous cases. The process was obviously accelerated: the hysteresis disappeared after only five thermal cycles (Fig. 8). The microstructural analysis, after the disappearance of the hysteresis, revealed that the grain boundaries were free of any carbides. These results indicate that oxygen penetration acts as an irreversible process to dissolve the grain boundary carbides, which leads to a stabilized peak P3 without hysteresis. This gives strong support to the above conclusions that peak P3 and the large
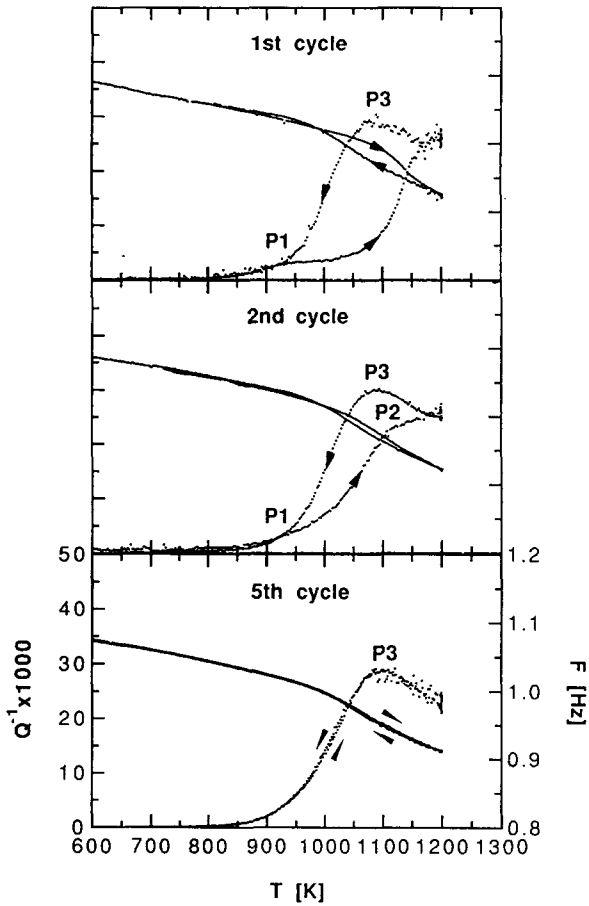
Fig. 8. Evolution of the internal friction spectrum Q^{-1} and frequency F measured on heating and cooling vs. temperature during different thermal cycles for Ni–22at.%Cr alloy, pre-oxidized in air for 1 h at 973 K.

hysteresis are related to grain boundary relaxation processes.

4. Discussion

The most important result in the present investigation is the experimental evidence which can prove the origin of grain boundary internal friction in Ni–Cr alloys. In particular, the behaviour of grain boundary internal friction is intimately related to the grain boundary microstructure.

It is known that the particles of a second phase may precipitate preferentially at grain boundaries and impede or block grain boundary relaxation [8, 10, 26]. Physically, this blocking effect arises from the internal stress produced by the particles impeding the boundary sliding [26]. Mori et al. [26] established a new model for grain boundary sliding and associated internal friction, taking into account the blocking effects of second-phase particles. According to these authors, when there is no diffusion around the blocking particles, the re-

laxation strength Δ is given by

$$\Delta = \Delta_0/(1 + \pi ar/\lambda^2) \qquad (1)$$

Here, Δ_0 is the relaxation strength when the boundaries are free from the second-phase particles; λ is the interparticle spacing; $2a$ is the grain size, and r is the radius of the blocking particles. It is obvious that the higher the size and the density of the particles are, the lower is the relaxation strength. It seems reasonable that both effects make the sliding more difficult and decrease the boundary mobility. With this point of view, it is possible to explain the grain boundary internal friction behaviour observed in Ni–Cr alloys.

The occurrence of the hysteresis (Fig. 1) is indicative of two states: (1) a low-temperature state with strong pinning points at the grain boundaries, leading to a low level of internal friction; (2) a high-temperature state associated with the decrease in the number or size of pinning points, leading to a high internal friction background. TEM observations [16] have revealed that the pinning points could be Cr_7C_3 carbide particles and ledges. These carbide particules can be considered as strong pinning points, regarding their size and their density at grain boundaries. Using the model of Mori et al., we can estimate approximately the blocking effect of Cr_7C_3 carbide particles in Ni–20at.%Cr. If we consider peak P3 as a grain boundary peak free of any carbide particles, and by taking $r = 0.5$ μm, $a = 40$ μm, $\lambda = 1$ μm and $\Delta_0 = 50 \times 10^{-3}$, we obtain $\Delta \approx 0.78 \times 10^{-3}$. This means that the Cr_7C_3 carbide particles block almost completely the grain boundary relaxation, which is in good agreement with the experimental results (Figs. 1 and 6).

Upon heating, the grain boundaries are strongly pinned by Cr_7C_3 carbide particles and no grain boundary motion is possible. Only the anelastic phenomena taking place within the grains, peak P1 related to Zener relaxation and an internal friction background are observed (Fig. 1). When the critical temperature of carbide dissolution is reached, the grain boundaries are denuded of second-phase particles and the boundary mobility increases abruptly, leading to macroscopic grain boundary sliding. As a result, a sharp increase in internal friction accompanied by a reduction in shear modulus is observed. During cooling, the grain boundary sliding is quite easy, with only the grain boundary ledges acting as pinning points, which leads to relaxation peak P3. As the boundary mobility is high, a high level of internal friction is observed. When the critical temperature of carbide precipitation is reached, the carbide particles appear simultaneously at grain boundaries, and the boundary mobility is suddenly decreased. Consequently, the grain boundary sliding is impeded again. Then, a significant decrease in internal friction, accompanied by an increase in shear modulus, is observed. Because

it occurs in the same temperature range as peak P1, peak P1 is effectively buried in the curve obtained upon cooling.

Indications of a similar hysteresis behaviour in internal friction have also been observed in molybdenum, owing to the precipitation and dissolution of extremely fine particles [27].

When the grain boundary is free of any carbide precipitates, the boundary mobility is high throughout the temperature range. Because no significant change occurs during the thermal cycles, a relaxation peak related to the steady mobility of grain boundary sliding is observed (*cf.* Fig. 7). In contrast, when the grain boundaries contain a high density of carbide particles, the particle blocking effect on grain boundary sliding is so strong that no grain boundary relaxation phenomena can be observed in the temperature range investigated, as shown in Fig. 8.

5. Conclusions

A high temperature internal friction relaxation peak, as well as a large hysteresis between heating and cooling cycles in the temperature range of the peak, are observed in Ni–Cr alloys. The origin of these phenomena are both related to grain boundaries. The relaxation peak can be explained by grain boundary sliding, which is affected by grain boundary carbide precipitates. The large hysteresis is attributed to the dissolution and precipitation of grain boundary carbides. We further conclude that internal friction measurements can be a useful method to study the dynamic process of grain boundary sliding.

Acknowledgments

References

1 M.H. Yoo, *Metall. Trans. A, 14* (1983) 547.
2 H.E. Evens, *Mechanism of Creep Fracture,* Elsevier, New York, 1984.
3 R. Raj, *Acta Metall., 26* (1978) 995.
4 H. Riedel, *Acta Metall., 32* (1984) 313.
5 H.J. Harris and G. Roberts, *Met. Forum, 4* (1981) 29.
6 C. Zener, *Phys. Rev., 60* (1940) 906.
7 T.S. Kê, *Phys. Rev., 71* (1947) 533.
8 D.R. Mosher and R. Raj, *Acta Metall., 22* (1974) 1469.
9 H. Gleiter, *High Angle Grain Boundaries,* Pergamon, Oxford, 1972, p. 233.
10 A.S. Nowick and B.S. Berry, *Anelastic Relaxation in Crystalline Solids,* Academic Press, New York, 1972.
11 G.M. Leak, *Proc. Phys. Soc., 78* (1961) 1520.
12 J.T.A. Roberts and P. Barrand, *J. Inst. Met., 96* (1968) 172.
13 G.M. Ashmarin, A.I. Zhikharev and Y.A. Shevedov, *IX. Conferencija Metaloznawcka PAN, Krakow, Poland, 1977,* p. 391, *Scr. Metall., 13* (1979) 801.
14 Z.Q. Sun and T.S. Kê, *J. Phys. (Paris), 42* (1981) C5-451.
15 J. Woirgard, J.P. Amirault and J. De Fouquet, in D. Lenz and K. Lücke (eds.), *Proc. 5th Int. Conf. on Internal Friction and Ultrasonicin Solids,* Vol. I, Springer, Berlin, 1975, p. 392.
16 A. Rivère and J. Woirgard, *Mater. Sci. Forum, 119–121* (1993) 125.
17 R. Schaller, J.J. Ammann and F. Cosandey, *J. Phys. (Paris), 48* (1987) C8-451.
18 F. Cosandey, J.J. Ammann, R. Schaller and W. Benoit, *Mater. Res. Soc. Symp. Proc., 122* (1988) 217.
19 F. Cosandey, S. Li, B. Cao, R. Schaller and W. Benoit, *Mater. Res. Soc. Symp. Proc., 229* (1991) 255.
20 B. Cao, R. Schaller, F. Cosandey and W. Benoit, *Mater. Sci. Forum, 119–121* (1993) 391.
21 J. Baur and A. Kulik, *J. Phys. (Paris), 44* (1983) C9-357.
22 K. Monma, H. Suto and H. Oikawa, *J. Jpn. Inst. Met., 28* (1964) 253.
23 B. Cao, R. Schaller, F. Cosandey and W. Benoit, in preparation.
24 R. Raj, *Acta Metall., 30* (1982) 1259.
25 B.F. Dyson, *Acta Metall., 30* (1982) 1639.
26 T. Mori, M. Koda and R. Monzen, *Acta Metall., 31* (1983) 275.
27 Y. Shiwa, H.P. Stüwe and E. Pink, *Acta Metall., 38* (1990) 819.